Resource-Efficient Parametric Recovery of Linear Time-Varying Systems

Andrew Harms*[1], Waheed U. Bajwa†[2], Robert Calderbank‡[3]
*Department of Electrical Engineering, Princeton University, Princeton, NJ, USA
†Department of Electrical and Computer Engineering, Rutgers University, Piscataway, NJ, USA
‡Department of Electrical and Computer Engineering, Duke University, Durham, NC, USA
[1]hharms@princeton.edu [2]waheed.bajwa@rutgers.edu [3]robert.calderbank@duke.edu

***Abstract*—This paper presents a novel, resource-efficient method of identifying the parametric description of linear, time-varying (LTV) systems, consisting of time shifts, frequency shifts, and complex amplitude scalings. Linear Frequency Modulation (LFM) waveforms are used to probe the system, and the returns are used to identify the parametric description. The number of samples required for perfect recovery is shown to scale linearly in the number of descriptive parameters K, and the sampling rate required is sub-Nyquist when compared to the bandwidth of the LFM waveforms. The time-bandwidth product of the LFM waveforms scales quadratically in K. Numerical examples demonstrate perfect recovery of closely spaced targets in the delay-Doppler space.**

I. Introduction

Identification of linear time-varying (LTV) systems has immediate application in radar and communication systems, among other areas. The identification is typically carried out by probing an LTV system with a known signal and processing the corresponding system output, which consists of several amplitude-scaled copies of the probing signal that are shifted in both time (delay) and frequency (Doppler). Traditional radar signal processing then employs matched filters which correlate the received signal against time and frequency shifts of the probe signal. Matched filtering (MF) is the maximum likelihood estimator for a single target (i.e., copy or return) in white Gaussian noise [1] but is limited by the spreading of the target peaks in the case of multiple targets. This spreading is captured in the ambiguity function (i.e., 2-D autocorrelation) of the probe signal and limits the resolution in the delay-Doppler space as targets in close proximity cannot be resolved due to the uncertainty principle.

Recent works have attempted to overcome the suboptimal nature of MF-based recovery, e.g., [2]–[5]. Many implicitly assume the time and frequency shifts lie on a discretized grid [2], [3]. Recently, [4] and [5] have proposed novel methods for identification of LTV systems that do not rely on the discretization of the parameters. Both utilize a two-stage procedure for recovery, which first recovers the time shifts and then uses that information to recovery the frequency shifts [5], or vice versa [4]. The sequential nature is a drawback because errors in the first stage can propagate to subsequent stages, as discussed in [4], [5]. In this paper, we revisit the problem of parametric recovery of LTV systems that neither relies on discretization of parameters nor uses a two-stage recovery procedure.

A. Our Contributions

For the probing waveform, our technique utilizes linear frequency modulated (LFM) waveforms, i.e., linear chirps that have the form

$$x(t) = e^{j2\pi(f_c t^2 + f_0 t)} g(t)$$

where $g(t) = 0 \ \forall t \notin [0, T_p]$ and is a unit-amplitude prototype pulse. The response of the LTV system to these waveforms, after some pre-processing, is a superposition of sinusoids with frequencies and phases determined by the time and frequency shifts describing the LTV system. If we also probe the system with a *negative* LFM waveform, i.e., with a negated exponent, then the time and frequency shifts can be recovered perfectly, in the absence of noise[1], through recovery of the frequencies and phases. In addition and in contrast to [5], we explicitly state the number of samples required for perfect recovery in the absence of noise, and show that the sampling rate is sub-Nyquist compared to direct sampling of the LFM waveform. We further show that the time-bandwidth product of the probing waveform needs to scale quadratically with the number of time/frequency shifts for perfect recovery.

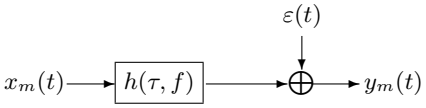

Fig. 1. Block diagram of the LTV system (1). A probing signal is time and frequency shifted prior to the addition of noise. In this paper $\varepsilon(t) \equiv 0$.

II. Parametric Description of an LTV System

An LTV system, shown in Fig. 1, is an operator consisting of K amplitude-scaled time shifts and frequency shifts. The response of the system to a probing signal $x(t)$ is

$$y(t) = \sum_{k=1}^{K} c_k x(t - \tau_k) e^{j2\pi f_k t} \tag{1}$$

for $t \in [0, \mathcal{T}]$ where $\mathcal{T}$ is the processing interval (during which the parameters are assumed fixed). Each component of the sum, indexed by k and referred to as a *reflector* return (referring to the physical interpretation), is parameterized by a distinct triplet (τ_k, f_k, c_k) corresponding to the time shift, frequency shift, and complex amplitude of each reflector. We assume that $f_k \in (-f_{max}, f_{max})$, $\tau_k \in [0, \tau_{max})$, and $|c_k| > 0 \ \forall k$.

III. Identification of an LTV System

Our goal is to identify an LTV system, i.e., recover the K triplets (τ_k, f_k, c_k), by processing the sampled response of the system to the probing signal $x(t)$ as *efficiently* as possible. Efficient recovery includes limiting the *number of samples*, the *size of the processing interval* $\mathcal{T}$, and the *time-bandwidth product* of $x(t)$.

A. Probing Waveform: Linear Frequency Modulation Pulses

In order to identify LTV systems, we propose the use of a train of LFM pulses, i.e., time-limited waveforms, as the probing waveform

$$x(t) = \sum_{m=0}^{M-1} x_m(t - mT) = \sum_{m=0}^{M-1} \left(x_m^+(t - mT) + x_m^-(t - mT) \right)$$

[1]Analysis of the noisy case will appear in a forthcoming journal paper.

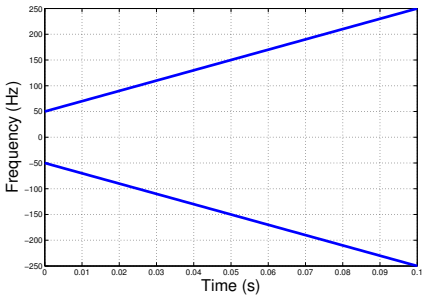

Fig. 2. Time-frequency plot of the LFM waveform with $f_0 = 50$ Hz, $f_c = 2000$ Hz/s, and $T_p = 0.1$ s.

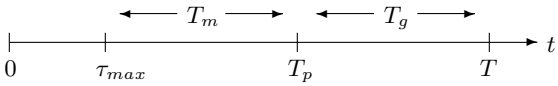

Fig. 3. Timing diagram of a pulse including the measurement and guard periods. We require that the guard period and pulse duration satisfy $T_g = T - T_p \geq \tau_{max}$ and $T_p > \tau_{max}$. The measurement period T_m has a lower bound that depends on the number of targets K.

where each pulse has a *positive* and *negative* component

$$x_m^{\pm}(t) = e^{\pm j2\pi(f_c^m t^2 + f_0^m t)} g(t)$$

and

$$g(t) = \begin{cases} 1, & 0 \leq t \leq T_p \\ 0, & \text{otherwise} \end{cases}$$

is a square pulse function of duration T_p and pulse repetition interval T. For the m^{th} pulse, f_c^m is the *chirp rate*, and f_0^m is the constant frequency offset. A time-frequency plot is shown in Fig. 2.

The received signal in the case of LFM pulses is

$$y(t) = \sum_{k=1}^{K} \sum_{m=0}^{M-1} c_k x_m(t - \tau_k - mT) e^{j2\pi f_k t} = \sum_{m=0}^{M-1} y_m(t)$$

where

$$y_m(t) = \sum_{k=1}^{K} c_k x_m(t - \tau_k - mT) e^{j2\pi f_k t}$$

is the received signal for the m^{th} pulse.

We require $T \geq T_p + \tau_{max}$ to ensure the received pulses $y_m(t)$ and $y_{m+1}(t)$ do not overlap. No signal is transmitted during the *guard interval* of duration $T_g = T - T_p$. An equivalent requirement for non-overlapping received pulses is $T_g \geq \tau_{max}$. We also restrict the measurements to the interval $t \in [mT + \tau_{max}, mT + T_p]$ to ensure all returns from the m^{th} pulse, and only those from the m^{th} pulse, are present. We term this interval the *measurement interval*, $T_m = T_p - \tau_{max}$. Fig. 3 provides a summary of the timing requirements.

Let $y_m(t) = y_m^+(t) + y_m^-(t)$ where $y_m^+(t)$ results from $x_m^+(t)$ and $y_m^-(t)$ results from $x_m^-(t)$. Expanding the positive component yields

$$y_m^+(t) = \sum_{k=1}^{K} c_k e^{j2\pi\{\theta_k^{m+} + \nu_k^{m+} t + (f_c^m t^2 + f_0^m t)\}} g(t - \tau_k)$$

where

$$\theta_k^{m+} = f_c^m \tau_k^2 - f_0^m \tau_k, \tag{2}$$
$$\nu_k^{m+} = f_k - 2 f_c^m \tau_k \tag{3}$$

are the phase offset and frequency of a sinusoid determined by the time and frequency shift of the k^{th} reflector. The negative component

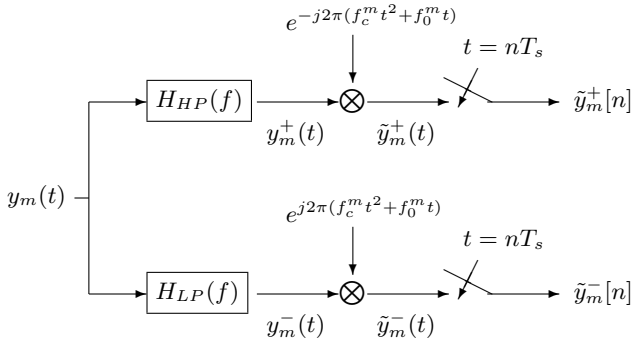

Fig. 4. The analog receiver processing filters, de-chirps, and samples the received signal prior to digital processing.

is expanded similarly with phase and frequency

$$\theta_k^{m-} = -f_c^m \tau_k^2 + f_0^m \tau_k = -\theta_k^{m+}, \tag{4}$$
$$\nu_k^{m-} = f_k + 2 f_c^m \tau_k. \tag{5}$$

The *pure chirp* part, $(f_c^m t^2 + f_0^m t)$, does not depend on any target.

B. Analog Processing and Sampling

Notice that $y_m^+(t)$ and $y_m^-(t)$ can be separated with appropriate filtering if $f_0^m > f_{max}$. A high-pass filter passes $y_m^+(t)$, and a low-pass filter passes $y_m^-(t)$. The receiver processing chain is shown in Fig. 4 where filtering is the first operation. For clarity of exposition, we concentrate on the positive component, with equal applicability to the negative component. After filtering, the received signal is *de-chirped* to remove the pure chirp component. The de-chirped signal is a sum of sinusoids with phases θ_k^{m+} and frequencies ν_k^{m+}:

$$\tilde{y}_m^+(t) = e^{-j2\pi(f_c^m t^2 + f_0^m t)} y_m^+(t) = \sum_{k=1}^{K} c_k e^{j2\pi\theta_k^{m+}} e^{j2\pi\nu_k^{m+} t} g(t - \tau_k). \tag{6}$$

This signal is then sampled over the measurement interval

$$\tilde{y}_m^+[n] = \tilde{y}_m^+(nT_s) = \sum_{k=1}^{K} c_k e^{j2\pi\theta_k^{m+}} e^{j2\pi\nu_k^{m+} nT_s} \tag{7}$$

for $n = 0, ..., N-1$, and T_s is the sampling period. The Nyquist criterion (to prevent aliasing) requires $2T_s \cdot (f_{max} + 2 f_c^m \tau_{max}) \leq 1$, or equivalently for the sampling rate $f_s = \frac{1}{T_s}$

$$f_s \geq 2(f_{max} + 2 f_c^m \tau_{max}). \tag{8}$$

Note that this Nyquist criterion is not related to the bandwidth of the LFM waveform, but to the size of the rectangle in the plane of time and frequency shifts determined by f_{max}, τ_{max}, and f_c^m.

IV. Parametric Recovery of an LTV System

Given the filtered, de-chirped, and sampled measurements (7), we first recover the frequencies and phases of the sinusoids and then extract the time and frequency shifts from the sinusoid frequencies and phases. We first ensure that the time shifts are unambiguously preserved in the phases of the sinusoids.

A. Ambiguous Phase Terms

The time shift-phase mapping (2) is a function of τ_k, so we write $\theta_k^{m+}(\tau_k)$ to highlight this. In order to invert $\theta_k^{m+}(\tau_k)$, it must 1) be bijective over $0 \leq \tau_k \leq \tau_{max}$ and 2) have a range contained in an interval of size at most 1 to prevent wrapping around the complex

unit circle. The following lemma provides necessary and sufficient conditions to prevent ambiguities. It applies to $\theta_k^{m-}(\tau_k)$ through (4).

Lemma 1 (Ambiguous Phase Terms)**.** *Let $0 \leq \tau_k \leq \tau_{max}$ and $f_c^m > 0$. The function $\theta_k^{m+}(\tau_k) = f_c^m \tau_k^2 - f_0^m \tau_k$ is bijective and $-1 \leq \theta_k^{m+}(\tau_k) \leq 0$ if and only if*

$$\frac{f_0^m \tau_{max} - 1}{\tau_{max}^2} \leq f_c^m \leq \frac{1}{2} \frac{f_0^m}{\tau_{max}} \tag{9}$$

and

$$f_0^m \leq \frac{2}{\tau_{max}}. \tag{10}$$

Proof. We know that a function is bijective on an interval if and only if it is strictly increasing or decreasing on that interval. We must ensure $\theta_k^{m+}(\tau_k) \in [a, b]$ with $|b - a| \leq 1$, and its derivative is non-negative (or non-positive) on $0 \leq \tau_k \leq \tau_{max}$. The rest of the proof is straightforward and omitted due to space constraints. □

B. Recovery Procedure for Time Shifts and Frequency Shifts

The need for the positive *and* negative chirp components is evident upon careful examination of (7). We can write $c_k = |c_k| e^{j\phi_k}$ and

$$\tilde{y}_m^+[n] = \sum_{k=1}^{K} |c_k| e^{j\psi_k^{m+}} e^{j2\pi\nu_k^{m+} n T_s} \tag{11}$$

with $\psi_k^{m+} = \phi_k + 2\pi\theta_k^{m+}$. Recovering ψ_k^{m+} and ν_k^{m+} is not sufficient to determine τ_k and f_k due to ϕ_k. However, the positive chirp paired with the negative chirp is sufficient. Using (4) and (5), we can write the received signal from the negative chirp similarly. The phases and frequencies of $\tilde{y}_m^+[n]$ and $\tilde{y}_m^-[n]$ are

$$\begin{aligned} \psi_k^{m+} &= \phi_k + 2\pi(f_c^m \tau_k^2 - f_0^m \tau_k), \\ \psi_k^{m-} &= \phi_k - 2\pi(f_c^m \tau_k^2 - f_0^m \tau_k), \\ \nu_k^{m+} &= 2\pi(f_k - 2f_c^m \tau_k), \\ \nu_k^{m-} &= 2\pi(f_k + 2f_c^m \tau_k). \end{aligned} \tag{12}$$

To recover the τ_k's and f_k's, we first recover the frequencies and phases (12) and then match the frequency–phase pairs from each processing chain. We finally invert the mapping $(\tau_k, f_k) \mapsto (\nu_k^{m+}, \nu_k^{m-})$ given by (3) and (5).

C. Frequency and Phase Recovery

We first recover the frequencies and phases from the samples (11); ψ_k^{m+} and ν_k^{m+} are recovered from $\tilde{y}_m^+[n]$ while, in parallel, ψ_k^{m-} and ν_k^{m-} are recovered from $\tilde{y}_m^-[n]$. We recover $\hat{\nu}_k^{m+}$ and $\hat{\nu}_k^{m-}$ using the Kumaresan-Tufts (KT) algorithm [6], but other parametric techniques such as MUSIC [7] or ESPRIT [8] would suffice.

The KT algorithm calculates the coefficients of a predictor filter

$$H(z) = z^L + h[1]z^{L-1} + \cdots + h[L-1]z + h[L]$$

with coefficients $h[a]$ for $a = 1, ..., L$ where L is the filter *predictor order*. Collecting the coefficients into a vector $\mathbf{h}$, we have $\mathbf{h} = -\mathbf{R}^{-1}\mathbf{r}$ where $\mathbf{R}$ is the data correlation matrix, and $\mathbf{r}$ is the data correlation vector. These are computed as follows.

For clarity, we denote generic measurements by $y[n]$ (for either $\tilde{y}^{m+}[n]$ or $\tilde{y}^{m-}[n]$). Build the *forward predictor* (Toeplitz) matrix

$$\mathbf{Y}^f = \begin{bmatrix} y[L] & y[L-1] & \cdots & y[1] \\ y[L+1] & y[L] & \cdots & y[2] \\ \vdots & \vdots & \vdots & \vdots \\ y[N-1] & y[N-2] & \cdots & y[N-L] \end{bmatrix},$$

backward predictor (Hankel) matrix

$$\mathbf{Y}^b = \begin{bmatrix} y^*[2] & y^*[3] & \cdots & y^*[L+1] \\ y^*[3] & y^*[4] & \cdots & y^*[L+2] \\ \vdots & \vdots & \vdots & \vdots \\ y^*[N-L+1] & y^*[N-L+2] & \cdots & y^*[N] \end{bmatrix},$$

and the forward and backward data vectors

$$\begin{aligned} \mathbf{y}^f &= [y[L+1]y[L+2]\cdots y[N]]^T, \\ \mathbf{y}^b &= [y^*[1]y^*[2]\cdots y^*[N-L]]^T. \end{aligned}$$

Finally, the forward-backward predictor matrix and vector are

$$\mathbf{Y} = \begin{bmatrix} \mathbf{Y}^f \\ \mathbf{Y}^b \end{bmatrix} \quad \text{and} \quad \mathbf{y} = \begin{bmatrix} \mathbf{y}^f \\ \mathbf{y}^b \end{bmatrix}.$$

The prediction equation is $\mathbf{y} + \mathbf{Y}\mathbf{h} = 0$. Solving for $\mathbf{h}$ yields $\mathbf{h} = -(\mathbf{Y}^H\mathbf{Y})^{-1}\mathbf{Y}^H\mathbf{y} = -\mathbf{R}^{-1}\mathbf{r}$ where $\mathbf{R} = \mathbf{Y}^H\mathbf{Y}$ and $\mathbf{r} = \mathbf{Y}^H\mathbf{y}$. The prediction filter $H(z)$ has L roots with K on the unit circle and $L - K$ inside. Let $\hat{z}_k$ denote the K roots recovered from the unit circle. The recovered frequencies $\hat{\nu}_k$ are found from $\hat{z}_k = e^{j2\pi\hat{\nu}_k T_s}$.

The phases $\hat{\psi}_k$ and amplitudes $|\hat{c}_k|$ are recovered by least-squares. Let F_ν be a Fourier matrix for frequencies $\hat{\nu}_k$ and defined by $[\mathrm{F}_\nu]_{n,k} = e^{j2\pi\hat{\nu}_k n T_s}$. Collecting the data into a vector $\tilde{y} = [\tilde{y}[0], ..., \tilde{y}[N-1]]^T$, the least-squares solution is defined as

$$\hat{\beta} = \arg\min_{\beta} ||\mathrm{F}_\nu \beta - \tilde{y}||_2^2$$

and the optimal solution $\hat{\beta}$ has entries

$$\hat{\beta}_k = |\hat{c}_k| e^{j\hat{\psi}_k}. \tag{13}$$

The procedure is summarized in Algorithm 1. The outputs ($\hat{\psi}_k^+$, $\hat{\psi}_k^-$, $\hat{\nu}_k^+$, and $\hat{\nu}_k^-$) are input to the time and frequency shift recovery.

Algorithm 1 Recovery of the frequency and phase of the sinusoids

1: Data: $y^{m+}[n]$ and $y^{m-}[n]$
2: **for** $r = \{+, -\}$ **do**
3: Calculate the predictor coefficients $\mathbf{h} = -\mathbf{R}^{-1}\mathbf{Y}^H\mathbf{y}$
4: Find the K roots of the prediction filter $H(z)$ with $|\hat{z}_k| = 1$.
5: Calculate the frequencies $\hat{\nu}_k^r = \frac{T_s}{2\pi}\arg(\hat{z}_k)$ from the roots $\hat{z}_k$.
6: Calculate the phases ψ_k^r and amplitudes $|c_k|$ from (13).
7: **end for**

D. Recovery of Time Shifts and Frequency Shifts

Recall that, due to the unknown phase term ϕ_k, knowledge of ψ_k^{m+} and ν_k^{m+} alone is not sufficient to determine τ_k and f_k. However, inclusion of the frequency and phase from the negative component provides sufficient information. Recovery of (12) provides K frequency-phase pairs from each processing chain. Each pair $(\hat{\psi}_k^{m+}, \hat{\nu}_k^{m+})$ must be matched with its counterpart from the other processing chain $(\hat{\psi}_k^{m-}, \hat{\nu}_k^{m-})$ for $k = 1, ..., K$.

To match the pairs, note the two relations

$$\frac{\nu_k^+ - \nu_k^-}{-8\pi f_c} = \tau_k, \tag{14}$$

$$\frac{\psi_k^+ - \psi_k^-}{4\pi} = f_c \tau_k^2 - f_0 \tau_k \tag{15}$$

where both quantities only depend on τ_k. Select two pairs indexed by k and ℓ, one from each processing chain, and compute a *hypothesized* delay from (14):

$$\tau_h(k, \ell) = \frac{\nu_k^+ - \nu_\ell^-}{-8\pi f_c}. \tag{16}$$

We then check if $\tau_h(k,\ell)$ satisfies (15) for k and ℓ, and if it does, we declare the *positive* pair k matched with the *negative* pair ℓ. Otherwise, we continue checking. This procedure is summarized in lines 1-10 of Algorithm 2.

With matched frequency-phase pairs from each processing chain, the recovered time and frequency shifts are

$$\hat{f}_k = \frac{\hat{\nu}_k^+ + \hat{\nu}_k^-}{4\pi} \quad \text{and} \quad \hat{\tau}_k = \frac{\hat{\nu}_k^+ - \hat{\nu}_k^-}{-8\pi f_c}. \tag{17}$$

The complex amplitude is recovered via (13):

$$\hat{\phi}_k = \frac{\hat{\psi}_k^+ + \hat{\psi}_k^-}{2} \quad \text{and} \quad |\hat{c}_k| = |\hat{\beta}_k|. \tag{18}$$

Algorithm 2 Recovery of the time and frequency shifts

1: Data: $\hat{\nu}_k^+$, $\hat{\psi}_k^+$, $\hat{\nu}_k^-$, and $\hat{\psi}_k^-$
2: Match frequency-phase pairs from each processing chain:
3: **for** $k = 1, ..., K$ **do**
4: **for** $\ell = 1, ..., K$ **do**
5: Calculate delay hypothesis (16).
6: **if** $f_c\tau_h(k,\ell)^2 - f_0\tau_h(k,\ell) = \frac{\psi_k^+ - \psi_\ell^-}{4\pi}$ **then**
7: Declare k matched with ℓ and exit.
8: **end if**
9: **end for**
10: **end for**
11: Detect and resolve ambiguous phases.
12: Calculate the time and frequency shifts (17) and amplitudes (18).

E. Sufficient Conditions for Recovery of Time and Frequency Shifts

The astute reader will note that the unknown phase terms ϕ_k can cause ambiguities in the recovery procedure, specifically in the matching of frequency-phase pairs. The following theorem establishes perfect recovery of the time and frequency shifts if a second pulse is transmitted, i.e., $M = 2$, to resolve these ambiguities.

Theorem 1 (Perfect Recovery of Time and Frequency Shifts)**.** *For a given τ_{max} and f_{max} and $M = 2$, choose $f_c^0 = -f_c^1 = f_c$, $f_0^0 > f_{max}$ and $f_0^1 = f_0^0 + f_c \cdot T_p$ satisfying Lemma 1. If f_s satisfies* (8) *and the number of samples N satisfies $N \geq K+1$, then Algorithms 1 and 2 perfectly recover the time shifts τ_k, frequency shifts f_k, and amplitudes c_k from the samples $\tilde{y}_m^{m+}[n]$ and $\tilde{y}_m^{m-}[n]$.*

We omit the proof due to space constraints and will provide it in a journal version. Fig. 5 shows the recovery, to machine precision, of a radar scene using the approach described in this paper including a magnified look at two closely spaced targets.

V. Discussion

A. Resource Usage

We highlight the advantages in resource usage of our approach, concentrating on 1) the rate and number of samples required for recovery and 2) the time-bandwidth product of the probing waveform.

1) Sampling rate and number of samples: To avoid aliasing, the sampling rate must satisfy the Nyquist condition (8), which is smaller than the rate required to sample an unprocessed LFM pulse (i.e., without de-chirping). An LFM pulse has bandwidth $W \approx \frac{1}{T_p} + f_c T_p$, and processing this signal directly (e.g., MF processing) requires a sampling rate of at least $2W$. In contrast, our approach requires the sampling rate (8). Recall that $T_m = T_p - \tau_{max}$ meaning $T_p > \tau_{max}$. Generally, $f_{max} < \frac{1}{T_p}$ as well, so our approach requires a lower sampling rate than a direct sampling of the LFM pulse.

Additionally, the KT algorithm requires a minimum number of samples, captured in Theorem 1, to recover the K frequencies, specifically $N \geq K+1$ samples. Recall that the measurements are acquired over time T_m, so we have the lower bound

$$T_m \geq \frac{N}{f_s}. \tag{19}$$

Further, T_p and T are determined by T_m. For a T_m satisfying (19), $T_p = T_m + \tau_{max} \geq \frac{N}{f_s} + \tau_{max}$ and $T = T_p + T_g \geq \frac{N}{f_s} + 2\tau_{max}$ where $T_g \geq \tau_{max}$ is the guard interval. The total processing time $\mathcal{T}$ needed for M pulses is $\mathcal{T} = M \cdot T$.

2) Time-bandwidth Product: Given the preceding discussion on $\mathcal{T}$ and W, the time-bandwidth product, $\mathcal{T} \cdot W$, of the LFM pulses is

$$\mathcal{T} \cdot W \approx M \cdot T \cdot \left(\frac{1}{T_p} + f_c T_p \right),$$

and $\mathcal{T} \cdot W$ must scale with $1 + K^2$.

B. Comparison to Other Parametric Techniques

Both [5] and [4] use sequential processing for recovery. In [5], the time shifts are first recovered followed by frequency shifts at each time shift, and vice-versa in [4]. In contrast, our approach requires only one recovery stage so errors do not propagate. Both [5] and [4] also require the transmission of a series of pulses. For [4], these pulses are stepped-frequency pulses, quite similar to an LFM pulse. The use of sequential processing requires an assumption on the maximum number of time shifts associated with any single frequency shift, which also affects the number of required samples for recovery. As a worst-case scenario, if there are K reflectors, then the minimum number of samples needed by [4] to recover the description is on the order of K^2. In contrast, the approach described in this paper requires the minimum number of samples to be on the order of K.

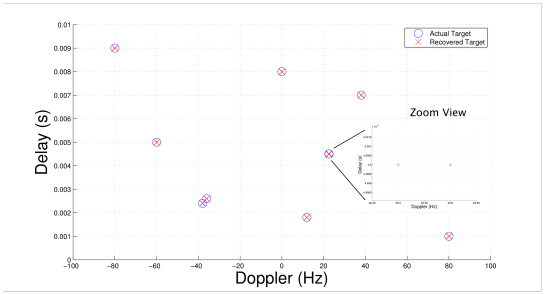

Fig. 5. Recovery of time and frequency shifts using the approach in this paper. The circles are the true shifts, and the crosses show the recovered shifts, which are recovered to machine precision. The zoom view shows recovery of two reflectors with the same time shift and very closely spaced frequency shifts.

References

[1] M. Skolnik, *Radar handbook*, 3rd ed. New York: McGraw-Hill, 2008.
[2] M. Herman and T. Strohmer, "High-resolution radar via compressed sensing," *IEEE Trans. Sig. Proc.*, 2009.
[3] X. Tan, W. Roberts, J. Li, and P. Stoica, "Range-doppler imaging via a train of probing pulses," *IEEE Trans. Sig. Proc.*, 2009.
[4] B. Friedlander, "An efficient parametric technique for doppler-delay estimation," *IEEE Trans. Sig. Proc.*, vol. 60, no. 8, 2012.
[5] W. U. Bajwa, K. Gedalyahu, and Y. Eldar, "Identification of parametric underspread linear systems and super-resolution radar," *IEEE Trans. Sig. Proc.*, 2011.
[6] D. W. Tufts and R. Kumaresan, "Estimation of frequencies of multiple sinusoids: Making linear prediction perform like maximum likelihood," *Proc. IEEE*, vol. 70, no. 9, pp. 975–989, 1982.
[7] R. O. Schmidt, "Multiple emitter location and signal parameter estimation," *IEEE Trans. Antennas Prop.*, vol. AP-34, no. 3, pp. 276–280, 1986.
[8] R. Roy and T. Kailath, "ESPRIT - estimation of signal parameters via rotational invariance techniques," *IEEE Trans. Acoust., Speech, Signal Proc.*, vol. 37, no. 7, pp. 984–995, 1989.